pISSN 2384-1095
eISSN 2384-1109

iMRI 2016;20:44-52

http://dx.doi.org/10.13104/imri.2016.20.1.44

iMRI
Investigative Magnetic Resonance Imaging

Improvement of Fat Suppression and Artifact Reduction Using IDEAL Technique in Head and Neck MRI at 3T

Jin Ho Hong, Ha Young Lee, Young Hye Kang, Myung Kwan Lim, Yeo Ju Kim, Soon Gu Cho, Mi Young Kim

Department of Radiology, Inha University Hospital, Inha University School of Medicine, Incheon, Korea

Purpose: To quantitatively and qualitatively compare fat-suppressed MRI quality using iterative decomposition of water and fat with echo asymmetry and least-squares estimation (IDEAL) with that using frequency selective fat-suppression (FSFS) T2- and postcontrast T1-weighted fast spin-echo images of the head and neck at 3T.

Materials and Methods: The study was approved by our Institutional Review Board. Prospective MR image analysis was performed in 36 individuals at a single-center. Axial fat suppressed T2- and postcontrast T1-weighted images with IDEAL and FSFS were compared. Visual assessment was performed by two independent readers with respect to; 1) metallic artifacts around oral cavity, 2) susceptibility artifacts around upper airway, paranasal sinus, and head-neck junction, 3) homogeneity of fat suppression, 4) image sharpness, 5) tissue contrast of pathologies and lymph nodes. The signal-to-noise ratios (SNR) for each image sequence were assessed.

Results: Both IDEAL fat suppressed T2- and T1-weighted images significantly reduced artifacts around airway, paranasal sinus, and head-neck junction, and significantly improved homogeneous fat suppression in compared to those using FSFS ($P < 0.05$ for all). IDEAL significantly decreased artifacts around oral cavity on T2-weighted images ($P < 0.05$, respectively) and improved sharpness, lesion-to-tissue, and lymph node-to-tissue contrast on T1-weighted images ($P < 0.05$ for all). The mean SNRs were significantly improved on both T1- and T2-weighted IDEAL images ($P < 0.05$ for all).

Conclusion: IDEAL technique improves image quality in the head and neck by reducing artifacts with homogeneous fat suppression, while maintaining a high SNR.

Keywords: IDEAL; Fat saturation; Head and neck MR; Susceptibility artifact; Metallic artifact

Original Article

Received: March 17, 2016
Revised: March 22, 2016
Accepted: March 22, 2016

Correspondence to:
Ha Young Lee, M.D., Ph.D.
Department of Radiology, Inha University College of Medicine, Inhangno 27, Jung-gu, Incheon 22332, Korea.
Tel. +82-32-890-2114
Fax. +82-32-890-2743
Email: pengoon@gmail.com

INTRODUCTION

The fat suppression technique is routinely used in clinical magnetic resonance imaging (MRI) of the head and neck to improve tissue or lesion contrast for characterization purposes (1). In head and neck MRI, abrupt changes in contour and density between air and soft tissue make magnetic inhomogeneity and susceptibility artifacts, which present as regions of signal loss and architectural distortion (1, 2).

Also, dental prostheses in the oral cavity cause metallic artifacts that are presented as signal voids surrounded by a peripheral rim of high signal intensity (3). These artifacts reduce image quality by causing architectural distortion, signal loss, and inhomogeneous fat suppression in the oral cavity, paranasal sinus (PNS), airway, and head-neck junction. Incomplete fat suppression and anatomical deterioration are commonly encountered in fat suppressed images obtained using the conventional frequency selective fat suppression (FSFS) technique, because FSFS is sensitive to magnetic field inhomogeneity and vulnerable to susceptibility and metallic artifacts.

Iterative decomposition of water and fat with echo asymmetry and least-squares estimation (IDEAL) technique using three asymmetric echo times and the three-point Dixon method for separating fat and water was introduced as an alternative solution for homogeneous fat suppression and reducing metal induced artifacts (4-14). Calculation of the quantity of magnetic field inhomogeneity in each pixel from data is applied to generate the field map of IDEAL, by using asymmetric echoes to prevent fat-water "swapping", which is frequently encountered using symmetric echoes, and by using the least-squares method. Phase shift is corrected in each pixel by using this field map, and images which accurately separate fat and water are generated (12, 15).

There are investigative reports which have been issued the usefulness of the IDEAL technique for the extremities and the spine (4-15). There was a technical report issuing the usefulness of IDEAL technique in separating fat and water in head and neck MR (16, 17), and a recent report presented a successful fat quantification using this technique in parotid glands (18). However, to our knowledge, there was no report on the application of IDEAL technique in the head and neck lesion in routine practical setting.

Thus, the purpose of our study was to prospectively compare the effectiveness of fat-suppressed (FS) T2- and postcontrast T1-weighted fast spine-echo (FSE) images using IDEAL to that using conventional FSFS with respect to metallic or susceptibility artifacts in the head and neck regions at 3T.

MATERIALS AND METHODS

Patients

This study was approved by our Institutional Review Board. and all subjects provided informed consent after receiving a full explanation of the nature of the study. We prospectively enrolled patients who were referred for head and neck evaluation using a 3-T MRI unit in our institution between September 2012 and August 2013. The exclusion criteria were as follows: (a) a scan range not including the oral cavity, and (b) MR images with severe motion artifacts affecting image interpretation. Sixty patients underwent the head and neck MR imaging during the period, and 24 patients were excluded due to severe motion artifacts. As a result, a total of 36 patients (23 men and 13 women; range, 24-85 years; mean, 55 years) were included in this study. Comparison of artifacts around the PNS, and oral cavity was possible in 21, and 30 patients, respectively, because these areas were not included in the cranial scan range in other patients. Pathologic diagnoses of the patients were as follows; malignancy in the oral cavity (n = 11), oropharynx (7), salivary gland (4), larynx (3) and hypopharynx (3), metastatic cervical lymphadenopathy (2), lymphoma (1), and benign lesions including lymphangioma (1), paraganglioma (1), AVM (1), venous malformation (1), and soft tissue edema (1).

MR Examination

MR examinations were conducted using a 3-T MRI system (Discovery 750W; GE Healthcare, Milwaukee, WI, USA) with a Geometry embracing method (GEM) head and neck coil suite. The scanner was a gradient system with 44 mT/m maximum gradient field strength and a 200 T/m/s slew rate. Axial IDEAL T2-weighted FSE and postcontrast axial IDEAL T1-weighted FSE images were taken in addition to our conventional contrast enhanced neck MRI images, which consisted of axial, coronal, and sagittal precontrast T1-weighted FSE, axial and coronal T2-weighted FSE, axial FSFS T2-weighted FSE, coronal short inversion time inversion-recovery (STIR) images, postcontrast axial, coronal and sagittal FSFS T1-weighted FSE, and axial diffusion weighted images. Table 1 summarizes the imaging parameters used in the study sequences. Contrast enhanced images were obtained after administering gadolinium-DTPA (Omniscan, GE Healthcare, Princeton, NJ, USA) (0.1 mmol/kg) into a cubital vein.

Image Analysis

Quantitative measurements were retrospectively performed by measuring the signal-to-noise ratio (SNR) on the picture archiving and communication system (PACS) viewer (Marosis, m-view 5.4; MAROTECH, Seoul, Korea) workstation. SNRs were measured in each imaging sequence

Table 1. Measurement Parameters for Study Sequences: IDEAL Fat Suppression T2-, IDEAL Postcontrast Fat Suppression T1-, Frequency Selective Fat Suppression (FSFS) T2-, and FSFS Postcontrast T1-Weighted Images

	IDEAL FS T2	IDEAL FS T1	FSFS FS T2	FSFS T1
TR/TE	5800/85	582/min full	4300/85	728/3
ETL	16	4	16	3
BW	62	62	35	31
ST/gap	3/0	3/0	3/0	3/0
FOV (mm)	18	18	18	18
Matrix size	288 x 224	288 x 192	320 x 160	288 x 160
Acquisition time	4:19	4:30	3:30	4:00

BW = bandwidth; ETL = echo train length; FOV = field of view; FS = fat suppression; FSFS = frequency selective fat suppression; IDEAL = iterative decomposition of water and fat with echo asymmetry and least-squares estimation; TE = echo time; TR = repetition time; W = weighted

at designated anatomical structures of four different levels; PNS, oral cavity, head-neck junction and mid-neck. The images bearing the largest part of maxillary sinus, the crown of first lower molar tooth, the body of hyoid bone, and the base of arytenoid cartilage were selected to represent PNS, oral cavity, head-neck junction, and mid-neck levels, respectively. For each representative image, circular regions of interest (ROI) were manually located by an single investigator (J.H.H. with 3 years of experience in head and neck imaging) over medulla oblongata or cervical spinal cord. The ROIs were drawn as large as possible to include homogeneous areas of designated structures. We compared the SNRs of each sequence to quantitatively assess the ability of IDEAL to maintain signal intensities. The SNR was calculated by dividing the signal intensity by the mean value of back-ground intensity (19), which was measured from the ROI outside the neck in a region free of artifacts.

Visual assessment of image qualities of two sets of sequences was retrospectively conducted: a) axial IDEAL FS T2-weighted, axial FSFS T2-weighted, and b) postcontrast axial IDEAL FS T1-weighted, and axial postcontrast FSFS T1-weighted images. All MR images from the 36 patients were independently reviewed by two head and neck radiologists (H.Y.L. with eight years and Y.H.K. with six years of experience). The readers were unaware of protocol information and image sets were presented in random order. Analysis of sets of images was performed using an independent PACS viewer.

Each category was evaluated using two different sets of MR sequences in the corresponding plane. The image qualities of categories were graded as follows:

a) The relative degree of metallic artifacts in the oral cavity

The degree of metallic artifacts from dental prosthesis, with respect to peripheral rim of high signal intensity, signal loss, and geographic distortion (20, 21), was graded as follows: grade 1, excellent image quality without significant artifact; grade 2, minimal degree of artifacts without significant image quality impairment; grade 3, moderate degree of artifacts with image quality impairment, but preserved diagnostic reliability; grade 4, severe artifacts resulting in limited diagnostic reliability; and grade 5, severe artifacts resulting in non-diagnostic image quality.

b) The relative degree of susceptibility artifacts around the upper airway, PNS, and head-neck junction

The degree of susceptibility artifacts with respect to signal loss and geographic distortion in three different sites of abrupt contour change or air-soft tissue interface were separately graded as follows: grade 1, excellent image quality without significant artifact; grade 2, minimal degree without significant image quality impairment; grade 3, moderate degree with image quality impairment, but preserved diagnostic reliability; grade 4, severe artifacts resulting in limited diagnostic reliability; and grade 5, severe artifacts resulting in non-diagnostic image quality.

c) Homogeneity of fat suppression

A section with the most inhomogeneous fat suppression in each set of protocols was selected, and graded as follows: grade 1, homogeneous fat suppression in whole image; grade 2, incomplete suppression in one quadrant; grade 3, incomplete suppression in two quadrants; grade 4, incomplete suppression in three quadrants; and grade 5, incomplete suppression in the whole image.

d) Contrast of lymph nodes/fat and of lesions/surrounding tissues

Overall contrast of each analytic item was graded as follows: grade 1, excellent; grade 2, good with minimal

image quality impairment; grade 3, moderate with some artifacts but still diagnostic; grade 4, poor with severe artifact resulting in limited diagnostic reliability; and grade 5, non-diagnostic.

e) Overall image sharpness

Image sharpness throughout images was graded as follows: grade 1, excellent; grade 2, good with minimal image quality impairment; grade 3, moderate with some artifacts but still diagnostic; grade 4, poor with severe artifact resulting in limited diagnostic reliability; and grade 5, non-diagnostic.

Statistical Analysis

All statistical calculations and tests were performed using SPSS ver. 19.0 (SPSS, Chicago, IL, USA). SNRs of IDEAL and FSFS sequences were compared by using the paired t-test. Results of qualitative analyses of two image sets were compared using the two-sided Wilcoxon's signed rank test for each individual reader. Interobserver agreements for the visual assessment of image qualities were assessed using the weighted κ statistic. The κ-values were interpreted as following; values less than 0.00 indicated poor agreement, between 0.00 and 0.20 indicated slight agreement, between 0.21 and 0.40 indicated fair agreement, between 0.41 and 0.60 indicated moderate agreement, between 0.61 and 0.80 indicated substantial agreement, and between 0.81 and 1.00 indicated almost perfect agreement. For all tests P values of < 0.05 were considered statistically significant.

RESULTS

The SNRs of medulla oblongata in PNS level, and SNRs of cervical cord in oral cavity, head-neck junction and mid-neck level were significantly higher both on IDEAL T2- and postcontrast T1-weighted images than that of FSFS T2- and postcontrast T1-weighted images ($P < 0.05$ for all). Table 2 summarizes the results of quantitative analysis.

Tables 3 and 4 show image quality scores for comparison of IDEAL and FSFS techniques on T2- and postcontrast T1-weighted images, respectively. Both IDEAL FS T2- and postcontrast T1-weighted images scored significantly

Table 2. Comparison of Mean Values of SNR between IDEAL and Frequency Selective Fat Suppression Sequences

	T2-weighted imaging			T1-weighted imaging		
	FSFS	IDEAL	P value	FSFS	IDEAL	P value
PNS	10.54 ± 4.92	70.66 ± 90.70	0.007	16.57 ± 10.13	78.08 ± 115.35	0.025
Oral cavity	8.22 ± 3.70	50.85 ± 43.64	< 0.001	3.90 ± 7.04	75.85 ± 80.61	< 0.001
HN junction	6.99 ± 3.08	57.43 ± 55.09	< 0.001	11.35 ± 4.29	85.90 ± 123.85	0.001
Mid-neck	6.61 ± 3.07	77.73 ± 69.30	< 0.001	10.38 ± 4.47	101.84 ±115.64	< 0.001

FSFS = frequency selective fat suppression; HN = head-neck; IDEAL = iterative decomposition of water and fat with echo asymmetry and least-squares estimation; PNS = paranasal sinus; SNR = signal-to-noise ratios

Table 3. Image-Quality Scores for IDEAL T2-Weighted Images and Frequency Selective Fat Suppression T2-Weighted Images

		Reader 1			Reader 2			κ-value
		FSFS	IDEAL	P value	FSFS	IDEAL	P value	
Metallic artifacts	Oral cavity	2.86 ± 1.00	2.43 ± 0.81	0.002	2.90 ± 1.02	2.60 ± 0.85	0.029	0.15
Susceptibility artifacts	Airway	2.88 ± 0.85	2.00 ± 0.33	< 0.001	2.55 ± 0.93	2.08 ± 0.55	0.006	0.11
	HN junction	3.80 ± 0.62	2.52 ± 0.60	< 0.001	2.63 ± 0.86	1.88 ± 0.57	< 0.001	0.10
	PNS	3.65 ± 0.81	2.10 ± 0.30	< 0.001	3.55 ± 0.94	2.10 ± 0.30	< 0.001	0.55
Homogeneous FS		4.30 ± 0.62	1.55 ± 0.60	< 0.001	3.66 ± 0.89	1.30 ± 0.70	< 0.001	0.28
Sharpness		2.72 ± 0.84	2.80 ± 0.40	0.433	2.86 ± 0.72	2.61 ± 0.54	0.079	0.16
Contrast	Lesion	2.41 ± 0.60	2.25 ± 0.43	0.058	2.25 ± 0.43	1.86 ± 0.48	0.029	0.12
	LN	2.33 ± 0.79	2.11 ± 0.46	0.070	2.11 ± 0.85	1.66 ± 0.47	0.002	0.20

HN = head and neck; FS = fat suppression; FSFS = frequency selective fat suppression; IDEAL = iterative decomposition of water and fat with echo asymmetry and least-squares estimation; LN = lymph node; PNS = paranasal sinus; W = weighted

better for homogeneous fat suppression by both readers (P < 0.001 for both), and IDEAL significantly reduced the relative degrees of artifacts around the airway, PNS, and head-neck junction (P < 0.05 for all) both on T2- and T1-weighted images. In addition, IDEAL FS T2-weighted images significantly decreased artifacts around the oral cavity (P

Table 4. Image-Quality Scores for IDEAL Postcontrast T1-Weighted Images and Frequency Selective Fat Suppression Postcontrast T1-Weighted Images

		Reader 1			Reader 2			κ-value
		FSFS	IDEAL	P value	FSFS	IDEAL	P value	
Metallic artifacts	Oral cavity	2.83 ± 1.01	2.50 ± 0.90	0.061	3.03 ± 1.06	2.56 ± 0.85	0.005	0.06
Susceptibility artifacts	Airway	2.75 ± 0.99	1.88 ± 0.46	< 0.001	2.58 ± 0.87	2.08 ± 0.60	0.004	0.25
	HN junction	3.75 ± 0.80	2.27 ± 0.56	< 0.001	2.88 ± 0.97	2.00 ± 0.63	< 0.001	0.28
	PNS	3.50 ± 0.94	2.10 ± 0.30	< 0.001	3.30 ± 0.92	3.30 ± 0.92	< 0.001	0.54
Homogeneous FS		3.97 ± 0.84	1.55 ± 0.77	< 0.001	3.11 ± 1.08	1.08 ± 0.28	< 0.001	0.18
Sharpness		2.77 ± 0.72	2.38 ± 0.54	0.010	2.69 ± 0.74	1.91 ± 0.43	< 0.001	0.18
Contrast	Lesion	2.25 ± 0.60	2.08 ± 0.60	0.034	1.97 ± 0.65	1.69 ± 0.52	0.026	0.14
	LN	2.33 ± 0.75	1.97 ± 0.44	0.003	1.91 ± 0.69	1.52 ± 0.50	0.004	0.20

HN = head and neck; FS = fat suppression; FSFS = frequency selective fat suppression; IDEAL = iterative decomposition of water and fat with echo asymmetry and least-squares estimation; LN = lymph node; PNS = paranasal sinus; W = weighted

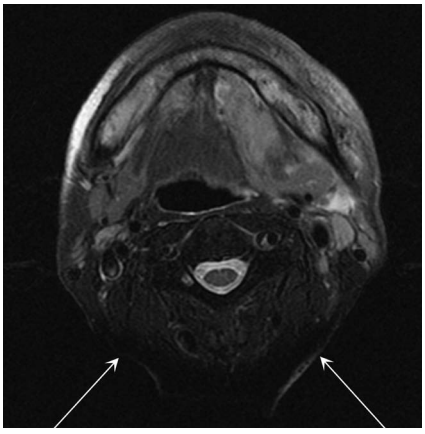

a

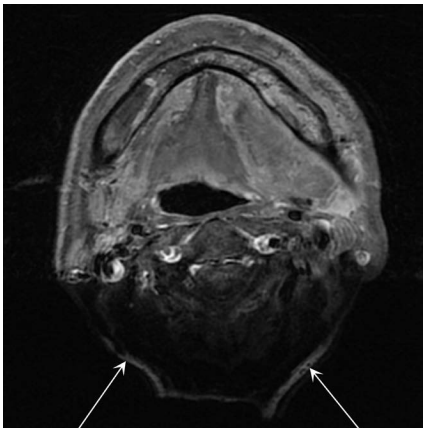

b

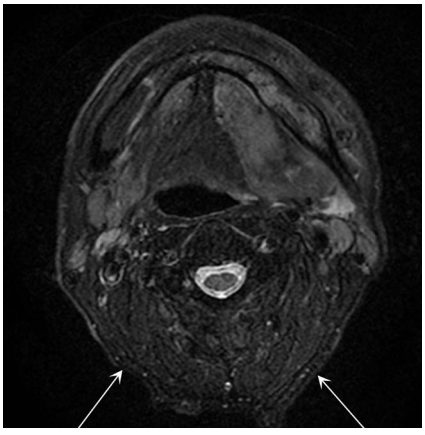

c

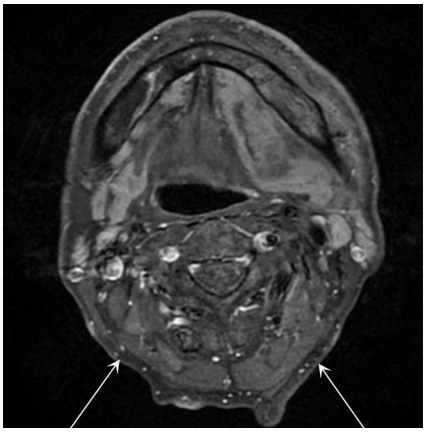

d

Fig. 1. MR images in a 56-year-old man with gingival cancer. Frequency selective fat suppressed T2- (a) and postcontrast T1-weighted (b) axial images show susceptibility artifacts identified as signal loss at the head-neck junction (arrows), obscuring normal anatomy. Corresponding IDEAL fat suppressed T2- (c) and T1-weighted (d) axial images show markedly less severe susceptibility artifacts and homogeneous fat suppression at the head-neck junction (arrows).

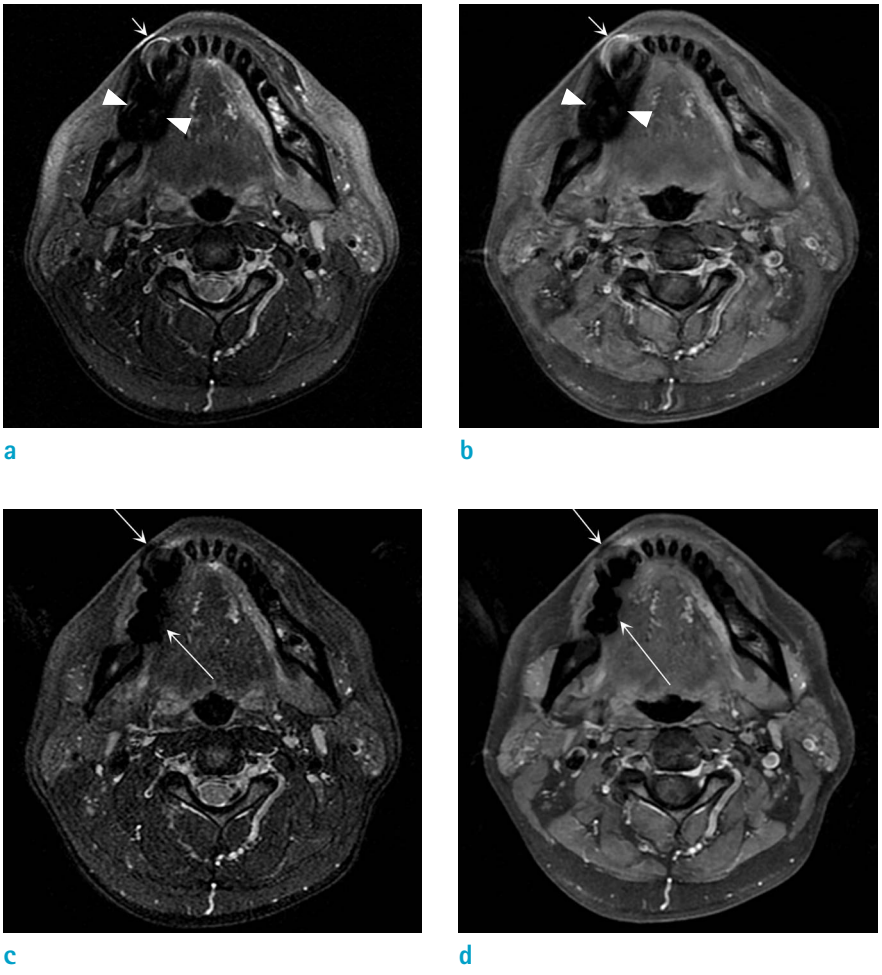

Fig. 2. MR images in a 47-year-old woman with paraganglioma. Frequency selective fat suppressed T2- (a) and postcontrast T1-weighted (b) images show metallic artifact, arising from a metallic crown identified as rim of high signal intensity (short arrows) and an area of low signal intensity (arrowheads) around the right anterior mandible body, obscuring adjacent gingiva, lip, and floor of mouth, and failed fat suppression. Marked reduction of metallic artifacts and homogeneous fat suppression are identified on corresponding IDEAL fat suppressed T2- (c) and T1-weighted (d) images (long arrows), improving the visibility of the surrounding anatomy.

= 0.002, 0.029, respectively) (Figs. 1-3). On FS postcontrast T1-weighted images, IDEAL significantly improved overall image sharpness, lesion-to-tissue contrast and lymph node-to-tissue contrast ($P < 0.05$, for all). Scores for lesion-to-tissue and lymph node-to-tissue contrast were better on IDEAL FS T2-weighted images, although there was no statistical difference in reader 1 ($P = 0.058$ and 0.070 for reader 1, $P = 0.029$ and 0.002 for reader 2, respectively). For both T2- and T1-weighted images, interobserver agreement between the two readers was moderate for susceptibility artifacts around PNS, and slight to fair for other categories.

DISCUSSION

Susceptibility artifacts and incomplete fat suppression are frequently encountered problems during MR evaluations of head and neck diseases (1, 22). The IDEAL technique was introduced as an alternative to provide homogeneous fat suppression and reduce metal-induced artifacts (4-12). Our study demonstrated that the IDEAL technique improved image quality by reducing metallic and susceptibility artifacts and by achieving more homogeneous fat suppression in head and neck 3-T MRI as compared with the FSFS method, while maintaining a high SNR.

Fat suppression techniques are routinely used during body MRI, especially T2-weighted and postcontrast T1-weighted imaging, which are essential for lesion detection and characterization in the head and neck, due to the large amounts of fat present in these regions (1, 2). The commonly used fat suppression methods are classified into 3 types; chemically selective methods: FSFS and water excitation (WE); inversion recovery methods: short T1 inversion recovery (STIR), spectral presuppression with inversion recovery (SPIR) and spectral adiabatic inversion recovery (SPAIR); and chemical shift based water-fat separation methods: Dixon methods including IDEAL (23-25). For head and neck MRI, abrupt changes in contour and

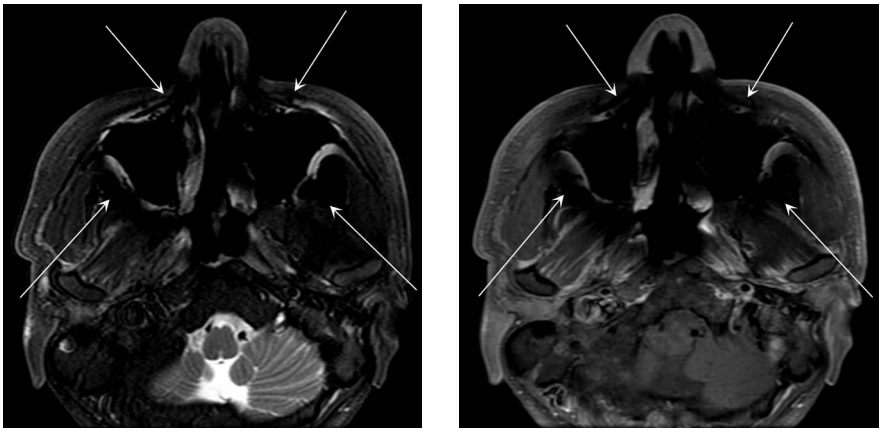

a b

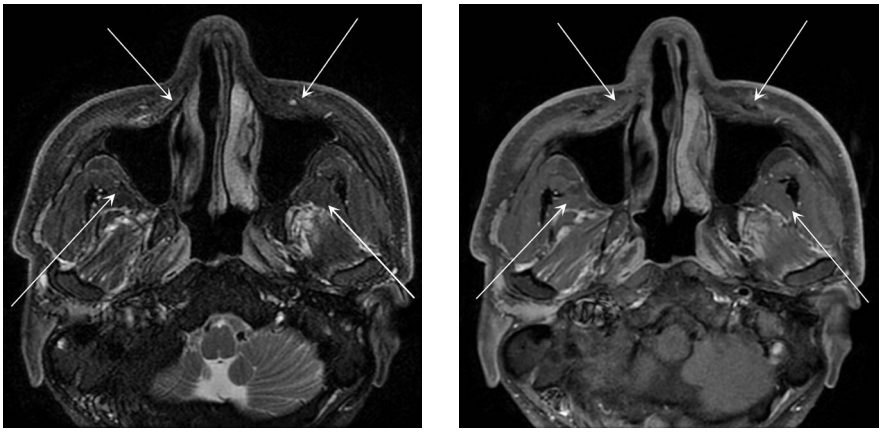

c d

Fig. 3. MR images in a 66-year-old man with buccal cancer. Areas of signal loss are seen around paranasal sinuses (arrows) due to susceptibility artifacts on frequency selective fat suppressed T2- (a) and T1-weighted (b) images. Corresponding IDEAL fat suppressed T2- (c) and T1-weighted (d) images show less severe susceptibility artifacts and improved visibility of the anatomy surrounding paranasal sinuses (arrows).

density between air and soft tissue cause inhomogeneity in the magnetic field (1, 2). This reduces image quality by architectural distortion, signal loss, and inhomogeneous fat suppression around the oral cavity, PNS, airway, and head-neck junction where substantial differences in magnetic susceptibility occur. Various metallic implants in oral cavity also cause field inhomogeneity and produce variable degrees of metallic and susceptibility artifacts (26). Conventional FSFS is sensitive to these artifacts, and STIR has been proposed as a solution of reducing susceptibility artifacts. However, STIR has several important limitations. STIR can only be combined with T2-weighted or proton density-weighted images, because it suppresses short T1 species with a T1 similar to that of fat, and thus, its use is limited with contrast media.

Several studies have reported on the usefulness of the IDEAL technique with respect to improving image quality by reducing artifacts in the extremities and spine (4-15). Previous reports have mentioned that the IDEAL technique improves visibility of the detailed anatomy (4-12), by enabling more homogeneous fat suppression and reducing tissue obscuring artifacts produced around metallic fixation devices in the spine. The IDEAL technique is relatively insensitive to both B0 and B1 inhomogeneity because it tracks background magnetic field variations, and thus, enables the reduction of metallic artifacts (11). In agreement with previous studies conducted in other body regions (4-12), IDEAL improved the image quality of head and neck MRI by reducing susceptibility and metallic artifacts, and producing more homogeneous fat suppression. In addition, we conducted objective analysis and demonstrated that IDEAL preserved higher SNR than FSFS.

In clinical practice, large areas of signal loss are frequently encountered around the head-neck junction airway and the PNS on FSFS T2-weighted and postcontrast T1-weighted images, and these cause significant distortion of the anatomy (1). In the present study, susceptibility artifacts and architectural distortion were markedly improved in

both IDEAL FS T2-weighted and postcontrast T1-weighted images, especially at the head-neck junction (Figs. 1, 2). Several studies have reported on the effectiveness of IDEAL for reducing the degrees of susceptibility artifacts around areas exhibiting abrupt contour changes in the extremities (12-14).

Metallic artifacts around metallic implants cause failed fat suppression and signal loss due to inadvertent water suppression caused by magnetic field inhomogeneity. These artifacts cause difficulties with the differentiation of failed fat suppression and true abnormal pathologic signal intensity. Metallic artifact is defined as areas of signal void surrounded by a rim of high signal intensity following the shape of a device (3). These artifacts are commonly encountered when conventional FSFS is used (1, 3). Many types of dental prostheses comprised of different materials are used in clinical practice, and these cause variable degrees of metallic artifacts that affect MRI quality in the head and neck. The extents of artifacts produced by dental prostheses depend on the type and quantity of metal (26-28). Gold and titanium display relatively mild artifacts, while stainless steel in arch bars, and lead and steel in dental crowns display severe in-plane and through-plane artifacts. Although, images were not analyzed with respect to component and type of dental prosthesis, IDEAL FS T2-weighted images significantly reduced the degrees of artifacts. Metallic artifacts were also significantly lower on postcontrast T1-weighted images according to one reader ($P = 0.005$). Intractable severe metallic artifacts caused by stainless steel, such as, arch bars and metal crowns, may not be improved by the IDEAL technique. The present study is the first to report the usefulness of the IDEAL technique for reducing metallic artifacts in the oral cavity, and suggests that the IDEAL technique provides a possible technical remedy for metallic dental artifacts.

Lesion/LN contrast and image sharpness were significantly improved on postcontrast IDEAL T1-weighted images, although they were not consistently improved on IDEAL T2-weighted images. Artifacts other than susceptibility and metallic artifacts also reduce image quality, such as, motion artifacts resulting from patient movement (29). A broad spectrum of artifacts due to pulsation, swallowing, and breathing occur even in the images of co-operative patients. Combination with other techniques that reduce motion artifacts, such as, PROPELLER or BLADE, with IDEAL may further enhance image quality by improving image sharpness and contrast-to-noise ratio.

There are several limitations in the present study. First, the study cohort was relatively small, as the study was conducted as a preliminary study to evaluate the feasibility of the IDEAL technique in the head and neck. Second, it was not possible to regulate motion artifacts, including swallowing and breathing during scanning, to exclude them as causes of poor image quality, and many cases were excluded due to severe motion artifacts. Furthermore, the extents of motion artifacts in the two protocols differed for all patients, because scanning could not be performed simultaneously. The patients with head and neck tend to be old, and the frequency of the movement during scan increases in those patients. Moreover, the total scan time of our study protocol was longer than our standard protocol to include IDEAL sequences for T2- and postcontrast T1-weighted images. Third, our study cohort was composed of patients with heterogeneous characteristics and underlying diseases. However, this is the first report to demonstrate the usefulness of the IDEAL technique for head and neck MRI. A multicenter study with a large homogeneous cohort may be necessary to confirm the usefulness of IDEAL.

In conclusion, IDEAL FS T2- and postcontrast T1-weighted images improved image quality by reducing artifacts around the airway, PNS, and head-neck junction, while maintaining high SNR, and provided homogeneous fat suppression of the head and neck facilitating accurate diagnosis. IDEAL may be a useful fat suppression method for the head and neck region in general practice.

Acknowledgments

This work was supported by Inha University Hospital Research Grant.

REFERENCES

1. Ross MR, Schomer DF, Chappell P, Enzmann DR. MR imaging of head and neck tumors: comparison of T1-weighted contrast-enhanced fat-suppressed images with conventional T2-weighted and fast spin-echo T2-weighted images. AJR Am J Roentgenol 1994;163:173-178
2. Finkenzeller T, Zorger N, Kuhnel T, et al. Novel application of T1-weighted BLADE sequences with fat suppression compared to TSE in contrast-enhanced T1-weighted imaging of the neck: cutting-edge images? J Magn Reson Imaging 2013;37:660-668
3. Petersilge CA, Lewin JS, Duerk JL, Yoo JU, Ghaneyem AJ. Optimizing imaging parameters for MR evaluation of the spine with titanium pedicle screws. AJR Am J Roentgenol 1996;166:1213-1218
4. Gerdes CM, Kijowski R, Reeder SB. IDEAL imaging of the

musculoskeletal system: robust water fat separation for uniform fat suppression, marrow evaluation, and cartilage imaging. AJR Am J Roentgenol 2007;189:W284-291

5. Chen CA, Lu W, John CT, et al. Multiecho IDEAL gradient-echo water-fat separation for rapid assessment of cartilage volume at 1.5 T: initial experience. Radiology 2009;252:561-567
6. Kijowski R, Woods MA, Lee KS, et al. Improved fat suppression using multipeak reconstruction for IDEAL chemical shift fat-water separation: application with fast spin echo imaging. J Magn Reson Imaging 2009;29:436-442
7. Grayev A, Shimakawa A, Cousins J, Turski P, Brittain J, Reeder S. Improved time-of-flight magnetic resonance angiography with IDEAL water-fat separation. J Magn Reson Imaging 2009;29:1367-1374
8. Murakami M, Mori H, Kunimatsu A, et al. Postsurgical spinal magnetic resonance imaging with iterative decomposition of water and fat with echo asymmetry and least-squares estimation. J Comput Assist Tomogr 2011;35:16-20
9. Cha JG, Jin W, Lee MH, et al. Reducing metallic artifacts in postoperative spinal imaging: usefulness of IDEAL contrast-enhanced T1- and T2-weighted MR imaging--phantom and clinical studies. Radiology 2011;259:885-893
10. Ren AJ, Guo Y, Tian SP, Shi LJ, Huang MH. MR imaging of the spine at 3.0T with T2-weighted IDEAL fast recovery fast spin-echo technique. Korean J Radiol 2012;13:44-52
11. Lee JB, Cha JG, Lee MH, Lee YK, Lee EH, Jeon CH. Usefulness of IDEAL T2-weighted FSE and SPGR imaging in reducing metallic artifacts in the postoperative ankles with metallic hardware. Skeletal Radiol 2013;42:239-247
12. Aoki T, Yamashita Y, Oki H, et al. Iterative decomposition of water and fat with echo asymmetry and least-squares estimation (IDEAL) of the wrist and finger at 3T: comparison with chemical shift selective fat suppression images. J Magn Reson Imaging 2013;37:733-738
13. Costa DN, Pedrosa I, McKenzie C, Reeder SB, Rofsky NM. Body MRI using IDEAL. AJR Am J Roentgenol 2008;190:1076-1084
14. Fuller S, Reeder S, Shimakawa A, et al. Iterative decomposition of water and fat with echo asymmetry and least-squares estimation (IDEAL) fast spin-echo imaging of the ankle: initial clinical experience. AJR Am J Roentgenol 2006;187:1442-1447
15. Reeder SB, Pineda AR, Wen Z, et al. Iterative decomposition of water and fat with echo asymmetry and least-squares estimation (IDEAL): application with fast spin-echo imaging. Magn Reson Med 2005;54:636-644
16. Barger AV, DeLone DR, Bernstein MA, Welker KM. Fat signal suppression in head and neck imaging using fast spin-echo-IDEAL technique. AJNR Am J Neuroradiol 2006;27:1292-1294
17. Ma J, Jackson EF, Kumar AJ, Ginsberg LE. Improving fat-suppressed T2-weighted imaging of the head and neck with 2 fast spin-echo dixon techniques: initial experiences. AJNR Am J Neuroradiol 2009;30:42-45
18. Chang HC, Juan CJ, Chiu HC, et al. Parotid fat contents in healthy subjects evaluated with iterative decomposition with echo asymmetry and least squares fat-water separation. Radiology 2013;267:918-923
19. Dietrich O, Raya JG, Reeder SB, Reiser MF, Schoenberg SO. Measurement of signal-to-noise ratios in MR images: influence of multichannel coils, parallel imaging, and reconstruction filters. J Magn Reson Imaging 2007;26:375-385
20. Tartaglino LM, Flanders AE, Vinitski S, Friedman DP. Metallic artifacts on MR images of the postoperative spine: reduction with fast spin-echo techniques. Radiology 1994;190:565-569
21. Laakman RW, Kaufman B, Han JS, et al. MR imaging in patients with metallic implants. Radiology 1985;157:711-714
22. Bellon EM, Haacke EM, Coleman PE, Sacco DC, Steiger DA, Gangarosa RE. MR artifacts: a review. AJR Am J Roentgenol 1986;147:1271-1281
23. Delfaut EM, Beltran J, Johnson G, Rousseau J, Marchandise X, Cotten A. Fat suppression in MR imaging: techniques and pitfalls. Radiographics 1999;19:373-382
24. Frahm J, Haase A, Hanicke W, Matthaei D, Bomsdorf H, Helzel T. Chemical shift selective MR imaging using a whole-body magnet. Radiology 1985;156:441-444
25. Ma J. Dixon techniques for water and fat imaging. J Magn Reson Imaging 2008;28:543-558
26. Shellock FG. MR imaging of metallic implants and materials: a compilation of the literature. AJR Am J Roentgenol 1988;151:811-814
27. New PF, Rosen BR, Brady TJ, et al. Potential hazards and artifacts of ferromagnetic and nonferromagnetic surgical and dental materials and devices in nuclear magnetic resonance imaging. Radiology 1983;147:139-148
28. Shellock FG, Morisoli S, Kanal E. MR procedures and biomedical implants, materials, and devices: 1993 update. Radiology 1993;189:587-599
29. Taber KH, Herrick RC, Weathers SW, Kumar AJ, Schomer DF, Hayman LA. Pitfalls and artifacts encountered in clinical MR imaging of the spine. Radiographics 1998;18:1499-1521